

Residual stress analysis in thick uranium films

A.M. Hodge^{a,*}, R.J. Foreman^b, G.F. Gallegos^b

^a *Materials Science and Technology Division, Lawrence Livermore National Laboratory, 7000 East Avenue, Livermore, CA 94550, USA*

^b *Manufacturing and Materials Engineering Division, Lawrence Livermore National Laboratory, 7000 East Avenue, Livermore, CA 94550, USA*

Received 17 December 2004; accepted 15 March 2005

Abstract

Residual stress analysis was performed on thick, 1–25 μm , depleted uranium (DU) films deposited on an Al substrate by magnetron sputtering. Two distinct characterization techniques were used to measure substrate curvature before and after deposition. Stress evaluation was performed using the Benabdi/Roche equation, which is based on beam theory of a bi-layer material. The residual stress evolution was studied as a function of coating thickness and applied negative bias voltage (0, –200, –300 V). The stresses developed were always compressive; however, increasing the coating thickness and applying a bias voltage presented a trend towards more tensile stresses and thus an overall reduction of residual stresses.

© 2005 Elsevier B.V. All rights reserved.

1. Introduction

Research on the physical, chemical and mechanical behavior of uranium (U) requires the use of advanced techniques such as X-ray Absorption Fine Structure (XAFS) and nanoindentation. These techniques require homogeneous samples, having uniform thicknesses in the 10–50 μm range, and in the case of nanoindentation, a mirror-like surface finish. Conventional machining of uranium presents a challenge when high precision parts are needed due to work-hardening under the slightest tool pressure [1], and the almost instant oxide layer formation [2]. Such requirements can be more achievable by using U films rather than machining parts from bulk materials. There are some studies in

the literature on physical vapor deposition (PVD) of U; these have focused on the substrate/coating diffusion layers with a very thin U layer (<1 nm) [3,4], or coating U to prevent oxidation [5]; however, the study of residual stresses in uranium films is an unexplored field.

Residual stress evolution in coatings has been an extensive area of research, mostly focusing on thin films (i.e., coating thickness \ll substrate thickness) [6,7] with some exceptions [8]. Residual stresses in physical vapor deposition films emerge from two factors: intrinsic stress during film growth and extrinsic stress due to thermal effects. For coatings deposited by PVD, changing coating parameters such as gas pressure, temperature, and applying a negative bias voltage to the substrate have been shown to change the stresses as well as the texture of the materials [9–11]. Currently, changes in PVD coating parameters and their effects on the coating structure are estimated by using the Thornton 4-zone diagram [8]; however, U is a complex material due to a highly

* Corresponding author. Fax: +1 925 422 6892.
E-mail address: hodge4@llnl.gov (A.M. Hodge).

anisotropic crystal structure, polymorphism, and a 5f electronic structure, and therefore it is not expected to behave as a typical metal film.

Techniques for measuring the deformation caused by the stresses developed during deposition fall into two categories: lattice based strain methods and surface curvature based methods. Lattice based methods such as X-ray diffraction present significant complexities for highly anisotropic materials such as uranium; therefore, surface curvature methods using profilometry are used. Previous studies on other metals have shown good accuracy for surface curvature methods [12]. Only small residual stress value deviations were found in thin coatings when comparing values calculated from X-ray diffraction techniques vs. laser curvature and profilometry techniques [13].

In this paper, to our knowledge, we present the first study of residual stresses in uranium coatings focusing on thick uranium coatings and including a study of the stress evolution as a function of applied negative bias voltage and film thickness. The overall surface deformation was measured using white light interferometry, stylus profilometry and the residual stress was calculated by the use of Benabdi/Roche (BR) equation, which is based on beam theory of a bi-layer material.

2. Experimental procedures

Films were prepared using a 33 mm diameter magnetron sputtering source, at 125 W power using a pressure of 10 mTorr and applying a negative bias voltage to the substrate of 0, –200 and –300 V. The substrate used was a 200 μm thick, lapped 25 mm diameter Al 1100–H112 disk. Substrates were heat treated to relieve stress due to lapping at 300 $^{\circ}\text{C}$ for 2 h and tested by Vickers microhardness. The Al substrates were cleaned before placing them in the vacuum chamber; while in the chamber, the substrate was ion milled for 30 s and then coated with ~ 30 nm of Ti for bonding purposes. Deposition times varied between 5 min and 4 h, depending on the desired film thickness. There were three substrates per coating run and a total of seven runs; two of the runs were used exclusively to check deposition rates. The substrate temperature was monitored during the deposition runs. Two distinct apparatus, a white light interferometer (Zygo NewView 5000, Middlefield, CT) and a stylus profilometer (Ambios XP, Santa Cruz, CA), were used to acquire the sample curvature profile before and after coating deposition. Scans were performed in four different directions, which were marked before coating; additionally, the markings were covered by a mask during the coating process in order to compare before and after profiles. The stylus profilometer and the scanning electron microscope (SEM) were used to determine coating thickness and surface roughness. After deposition, den-

sity measurements were performed on the coated samples by the Archimedes method using FC-43 as the fluid.

3. Results and discussion

3.1. Coating characterization

Extensive efforts were made to characterize the samples the same day that the coating was completed in order to minimize any effects due to oxidation. Density tests show the DU coatings to be greater than 99% dense when compared to the theoretical density of U (19.4 g/cm^3). Furthermore, characterization performed by SEM show that all coatings appear to have a smooth interface to the substrate; EDS analysis confirmed that there were only U peaks at the substrate/coating boundary. There is no evidence of an intermetallic layer by EDS analysis; however, a faint signal detected at the highest magnifications suggested the presence of Ti. X-ray diffraction performed on the U films show a highly textured sample with only U peaks present.

Fig. 1(a) depicts a SEM micrograph of a representative cross-section of the U coating, which shows a homogeneous coating throughout the sample. Coating thickness was also measured with the stylus profilometer by scanning the step height between the mask and un-masked region. The coating had a smooth, mirror-like surface and is made up of dense fiber-like grains, as

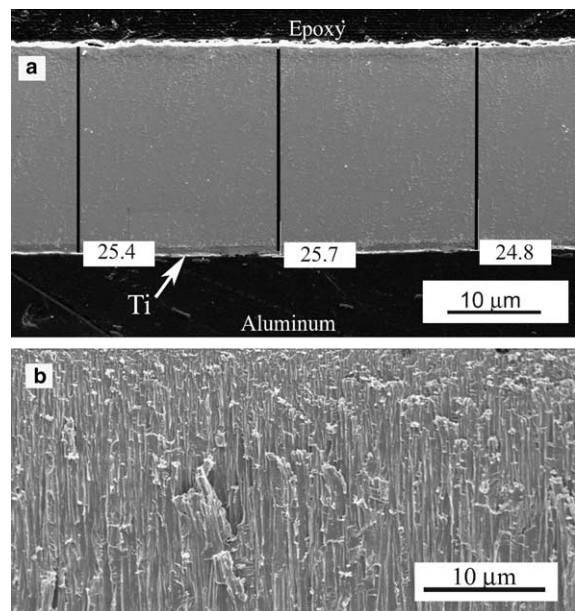


Fig. 1. SEM micrographs of (a) polished and coated surface showing uniform coating thickness and (b) coating fracture surface showing dense fiber-like grains.

can be seen in Fig. 1(b), which shows a typical unpolished fracture surface of the coating. This particular coating structure was described by Thornton and Hoffman [14] and is considered to be in 'region T ', which is the transition region and is known to form large intrinsic stresses. Overall, the microstructure of the uranium coatings seems to fit well when compared to the predicted microstructure based on argon pressure vs. T/T_m Thornton diagram (where T is the substrate temperature and T_m is the melting temperature of the coating); for this case, $P = 10$ mTorr and $T/T_m = 0.2$. To our knowledge, this is the first time that uranium has been shown to fit the predicted structure. Use of the Thornton diagram would allow selective changes in the coating microstructure by changing the coating parameters.

Fig. 2(a) shows 20 mm long scan lines A, B, C, and D taken by white light interferometry. Smaller scans (2 mm) were performed at the edge of the mask/unmasked region for a total of eight measurements for thickness for each sample. The standard deviation for the thickness was less than $1 \mu\text{m}$ at any given scan for the 20–25 μm thick coatings. Fig. 2(b) shows a plot of the before- and after-coating profile for line C, run 3; for this particular disc line C had the highest deflection. Note that the diameter is in mm and the total deflection is in microns. The maximum deflection (δ_{max}) of scans A, B, C and D are averaged to show the average highest deflection for each disc. Similar plots were done for each scan line before and after coating; the profile before coating was subtracted from the profile after coating to give the total deflection. The peak of the deflection is right at the center of the disk and it is labeled as δ_{max} . Deflection measurements were performed by white light interferometry.

Table 1 presents a summary of the average of the maximum deflection (δ_{max}) from line scans A, B, C,

Table 1
Deflection and thickness measurements from white light interferometry and profilometry

Coating #	Bias (V)	Coating thickness (μm)	δ_{max} average (μm)
1	0	24.8	700
2	0	20	700
3	-200	20.6	435
4	-300	23.7	435
5	-300	26.4	383

and D at a given thickness. Note that the diameter of the coated area was 20 mm for all samples, so the δ_{max} shows a real decrease as a function of substrate bias.

The use of stylus profilometry and white light interferometry allows us to obtain accurate measurements for total disc deformation and film thickness; these values provide the necessary parameters to calculate the residual stresses. SEM measurements were used to verify the coating thickness values.

3.2. Residual stress equations

Since our measurements are performed ex situ, the residual stresses presented here are the total stresses due to intrinsic and extrinsic factors. In this particular work, we will make the assumption that there is no in-plane deformation of the coated surface, i.e., the deflection is caused only by the free contraction or elongation of the coating layer [15]. This narrows the available residual stress equations to the Stoney (Eq. (1)), Röll (Eq. (2)) and Benabdi/Roche (BR) (Eq. (3)) equations [15–17]. The three equations mentioned also assumed a constant residual stress distribution over the whole coating; this is a valid assumption because our film/substrate

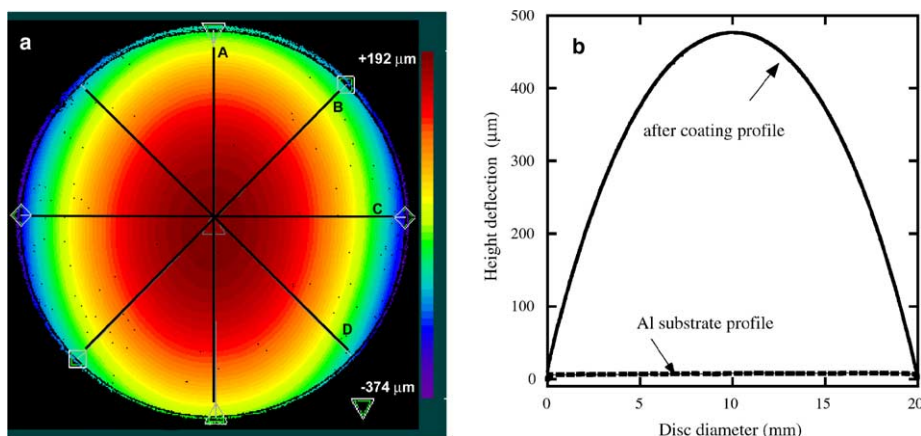


Fig. 2. White light interferometry from sample 5 coated using -300 V bias: (a) scan lines A, B, C, D and (b) deflection profile before and after coating for scan line C.

thickness ratio is $\sim 13\%$. Eqs. (1)–(3) have been further modified to include a bi-axial modulus as suggested by Timoshenko [18].

$$\sigma_{\text{Stoney}} = \frac{-E_s \cdot t_s^2}{6 \cdot t_c \cdot (1 - \nu_s) \cdot R}, \quad (1)$$

$$\sigma_{\text{Röll}} = \frac{-E_s \cdot t_s^2}{6 \cdot t_c \cdot (1 - \nu_s) \cdot R} \cdot [1 + \beta(4\gamma - 1)], \quad (2)$$

$$\sigma_{\text{BR}} = \frac{-E_s \cdot t_s^2}{6 \cdot t_c \cdot (1 - \nu_s) \cdot R} \cdot \left[1 + \beta(4\gamma - 1) + \beta^2 \cdot \left[\gamma^2 \cdot (\beta - 1) + 4\gamma + \frac{(1 - \gamma)^2}{1 + \beta} \right] \right], \quad (3)$$

where:

$$\gamma = \frac{E_c(1 - \nu_s)}{E_s(1 - \nu_c)},$$

$$\beta = \frac{t_c}{t_s},$$

$$R = \frac{L^2}{8 \cdot \delta_{\text{max}}},$$

where R is the radius of curvature, L is the length of the coating (20 mm), and δ_{max} is the maximum deflection. Additionally, c denotes coating and s denotes substrate.

Most of the current literature addressing stress analysis focuses on thin films for which Stoney's equation is widely used; however, this equation has a valid thickness ratio (t_c/t_s) limit of $\sim 5\%$ of the coating thickness [6]. As can be seen in Eq. (1), Stoney's equation takes into account the Elastic Modulus and Poisson ratio of the substrate only. However, as the film thickness approaches the substrate thickness, there are multiple parameters from the coating that must be taken into account in order to accurately calculate the residual stresses. The main difference between Eqs. (1)–(3) is the addition of higher order terms which is discussed elsewhere [15].

For thick coatings, there are multiple factors which affect the stress behavior and are a combination of the coating and substrate properties. One example is the ratio α , which is the ratio of the elastic modulus of the coating and the substrate (E_c/E_s). There are multiple configurations for α such as: compliant substrate/compliant coating ($\alpha = 1$), stiff substrate/stiff coating ($\alpha = 1$), compliant coating/stiff substrate ($\alpha \ll 1$), and stiff coating/compliant substrate ($\alpha \gg 1$). In the case of an aluminum substrate coated with U, $\alpha \approx 3$, which will be considered as compliant coating to a compliant substrate.

As can be seen in Eq. (3), the BR equation includes additional higher order terms to account for the coating thickness and properties. Stresses were calculated using all three equations for a thin film 1μ thick, and all three equations gave the same result. However, since we are interested in films $\sim 25 \mu$ thick, we have selected to

use only the BR equation, which was derived to work for thin and thick coatings. All stress values presented throughout this paper have been calculated using BR equation.

3.3. Residual stress results

Fig. 3 shows the residual stress values of the uranium coatings as a function of film thickness. At our target thickness of $25 \mu\text{m}$, a residual stress of -1.0 GPa was calculated, which is noticeably less than the residual stress of -3.5 GPa calculated for the $1 \mu\text{m}$ thick film. No attempts were made to make thicker coatings since our U source has a constant coating rate for the first 4 h but seems to degrade after longer periods. This allows us to predict the coating thickness. Note that as the coating thickness increases, the stress becomes less compressive. However, at $25 \mu\text{m}$ film thickness, the residual stress is close to -1.0 GPa , which is high; therefore, changes in the coating parameters (the addition of a negative bias voltage) had to be introduced in an attempt to lower the residual stresses. Fig. 4 shows a reduction of residual stresses by introducing a bias voltage. We were able to reduce the stresses by over half by applying a bias voltage. The most significant reduction in stress occurred at -200 V . The -300 V coating run had a more modest decrease compared to the -200 V bias run; furthermore, it showed a large deviation in stress distribution for scans A, B, C and D. Due to machine limitations, coatings using negative bias voltage beyond 300 V were not performed.

In this particular study we encountered two major unknown factors that played a significant role in the coating behavior: the complex crystal structure of U, and the coatings thickness. Literature on thick films

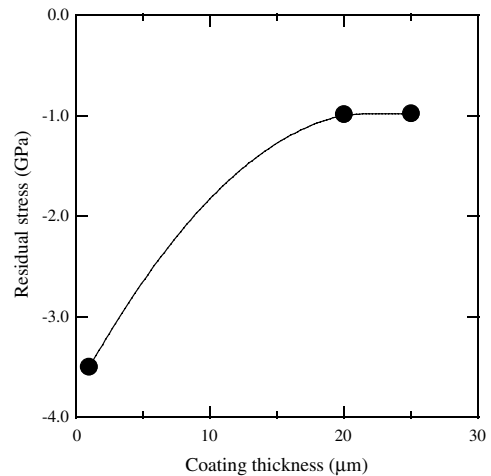


Fig. 3. Calculated residual stresses using BR equation as a function of coating thickness (without bias).

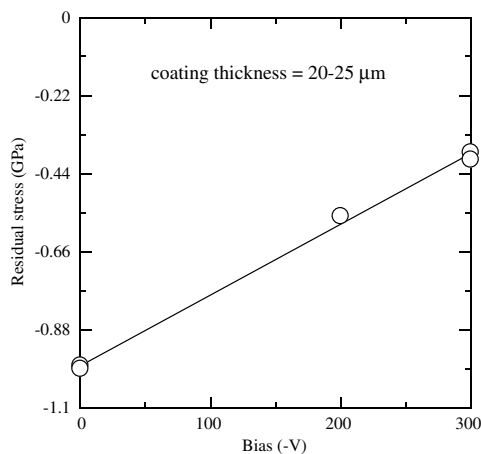


Fig. 4. Residual stress as a function of bias voltage at coating thickness of $\sim 25 \mu\text{m}$ (note that there are two distinct data points at 0 V and at -300 V).

($25 \mu\text{m}$) is very sparse with few exceptions [8,19]. Current research on sputtered films deposited with a bias voltage is based mostly on thin films ($<300 \text{ nm}$) with FCC and BCC structures. Patten et al. study the effects of a small substrate bias (-70 V) on the microstructure of thick Cu and Cr films (up to 1.0 mm) [19,20], however there is no measure of residual stresses. For thin films, there are a few samples of the effects of bias on the residual stresses. Cheng et al. [9] deposited 250 nm of Cu on (100) silicon wafers and applied a negative bias voltage from -50 to -600 V . They observed that, as the bias voltage increased, the residual stress changed from 200 MPa at 0 V to -300 MPa at 600 V , so the coating became compressive as the bias voltage was increased. Cr coatings of 150 nm thickness show a similar behavior to the Cu; as bias increased to -500 V , the residual stress became compressive going from 1.0 to -2.2 GPa [11]. Effects of the bias on the film roughness were small and did not present a trend, as shown by other researchers [9,21].

The effect of the bias on thin films is due to the increase of energetic particles, which causes an 'atom peening mechanism' and explains the transition from tensile to compressive stress [11,14]. It would be difficult to explain why the uranium films become less compressive as the bias is increased without additional data. The atom peening mechanism still applies but perhaps other mechanisms are more dominant. It has been shown in many metals that when a substrate bias is applied, the texture of the films changes [9,11,21]. The texture can then be related to changes in microstructure and film properties such the elastic modulus and yield strength which are related to increase/decrease in the films intrinsic residual stresses [22,23]. Uranium films have additional issues which can further affect the stress evolution. First,

depending on texture, the coefficient of thermal expansion in U can be drastically different [24], thus changing the contribution of the extrinsic stresses on the total stress value. Another unknown is the in situ stress as the coating is formed; as the plasma temperature increases, there is an influx of atoms that can form α -, β -, or γ -uranium, which would affect the intrinsic stresses of the coating. Once the PVD process is completed, the film is α -U but, if the coating is initially a different phase, the transition from one phase to α U can produce additional stress to the coating.

In order to fully understand the origins of the intrinsic stresses in U studies using in situ monitoring of the stress evolution must take place. Additionally, further investigations of the U phase transition during PVD would allow a very complete assessment on the formation of residual stresses.

4. Conclusions

We have successfully produced thick uranium coatings ($25 \mu\text{m}$) on an Al substrate. The coatings adhere well to the substrate and are characterized as fully dense with homogeneous thickness throughout the length of the coating. The film deflection was measured by profilometry and the stresses calculated using the Benabdi/Roche equation. The residual stresses were presented as a function of thickness and applied negative bias voltage. The stresses measured were always compressive; however, increasing the coating thickness and adding a bias voltage presented a trend towards more tensile stresses and thus an overall reduction of residual stresses.

Acknowledgements

This work was performed under the auspices of the U.S. Department of Energy by the University of California, Lawrence Livermore National Laboratory under Contract No. W-7405-Eng-48. The authors thank L. Cook, J. Lotscher, R. del Chiaro and E. Sedillo at LLNL for sample preparation and characterization, and Mr P. O'Hara at Ambios Technology, Inc. for helpful discussions.

References

- [1] W.D. Wilkinson, Uranium Metallurgy, vol. I, Interscience Publishers, New York, 1962.
- [2] J.V. Cathcart, in: J.J. Burke et al. (Eds.), Physical Metallurgy of Uranium Alloys, Brook Hill Publishing Company, Massachusetts, 1976, p. 775.
- [3] T. Gouder, C.A. Colmenares, Surf. Sci. 295 (1993) 241.

- [4] T. Gouder, C.A. Colmenares, Surf. Sci. 295 (1994) 241.
- [5] X. Xiaobin, L. Kezhao, L. Xuechao, Z. Yongbin, Rare Met. Mater. Eng. 32 (2003) 67.
- [6] L.B. Freund, S. Suresh, Thin Film Materials: Stress, Defect Formation and Surface Evolution, Cambridge University, Cambridge, 2003.
- [7] W.D. Nix, Met. Trans. 20A (1989) 2217.
- [8] J.A. Thornton, J. Vac. Sci. Technol. 11 (1974) 666.
- [9] Y.H. Cheng, B.K. Tay, S.P. Lau, X. Shi, H.S. Tan, J. Vac. Sci. Technol. 19A (2001) 2102.
- [10] M. Oden, J. Almer, G. Hakansson, Surf. Coat. Technol. 10 (1999) 39.
- [11] A. Misra, M. Nastasi, Appl. Phys. Lett. 75 (1999) 3123.
- [12] J. Gunnars, U. Wiklund, Mater. Sci. Eng. 336A (2002) 7.
- [13] Z.B. Zhao, J. Hershberger, S.M. Yalisove, J.C. Bilello, Thin Solid Films 415 (2002) 21.
- [14] J.A. Thornton, D.W. Hoffman, Thin Solid Films 171 (1989) 5.
- [15] M. Benabdi, A.A. Roche, J. Adhes. Sci. Technol. 11 (1997) 281.
- [16] K. Roll, J. Appl. Phys. 47 (1976) 3224.
- [17] G.G. Stoney, Proc. R. Soc. London 82A (1909) 172.
- [18] S. Timoshenko, J. Opt. Soc. Am. 11 (1925) 233.
- [19] J.W. Patten, E.D. McClanahan, J.W. Johnston, J. Appl. Phys. 42 (1971) 4371.
- [20] J.W. Patten, E.D. McClanahan, J. Appl. Phys. 43 (1972) 4811.
- [21] C. Gautier, G. Moulard, J.P. Chatelon, G. Motyl, Thin Solid Films 384 (2001) 102.
- [22] A. Misra, M. Nastasi, J. Mater. Res. 14 (1999) 4466.
- [23] M. Janda, O. Stefan, Thin Solid Films 112 (1984) 127.
- [24] L.T. Lloyd, C.S. Barrett, J. Nucl. Mater. 18 (1966) 55.